

direction of cardiac looping. The similarity of the cardiac and pulmonary phenotypes of *Pitx2*^{-/-} and *ActRIIB*^{-/-} (ref. 17) indicates that *Pitx2* is the critical downstream target of *ActRIIB*, a putative Nodal receptor, mediating effects on both cardiac positioning and pulmonary isomerism. The *Pitx2* phenotype extends to tissues other than those affected by *ActRIIB*, indicating that *Pitx2* gene activation may be controlled separately in these tissues. *Pitx2* is thus, to our knowledge, the first transcription factor that can be considered to be a critical component in mediating the proliferative/motility events of the lateral-plate mesoderm that underlie ventral body-wall closure and 'leftness' in lung patterning and organ placement, as well as serving critical later roles in organogenesis. □

Methods

Generation of *Pitx2*-knockout mice.

Genomic clones encompassing the entire *Pitx2* transcript were obtained from the 129/SvJ mouse genomic library (Stratagene). The 5'-arm is a 5.0-kilobase (kb) *NdeI*-*Ngo*MI fragment bordering the DNA-binding domain and the 3'-arm is a 4.5-kb *Bam*HI-*Sall* 3'-end fragment that includes the entire 3' untranslated region. The region from the homeodomain to the C-terminus of *Pitx2* is replaced by the *LacZ/neo*mycin sequences, driven by the *Pitx2* promoter. R1 embryonic stem cells were grown and selected with G418 and gancyclovir, and Southern blot analysis was carried out using a 5'-external (1.6-kb) probe that hybridizes to a 8-kb *Kpn*I wild-type and a 6-kb *Kpn*I/*Bam*HI recombinant band. We confirmed genotyping of heterozygotes and homozygotes using a 3'-internal (0.6-kb) probe that recognizes a 3.6-kb *Pst*I fragment in the wild-type and a 2.8-kb *Pst*I fragment in the recombinant alleles.

In situ hybridization, whole-mount hybridization and *LacZ* staining.

Isolation, fixation, and hybridization with ³⁵S-labelled antisense RNA probes and exposure were done as described¹. For whole-mount in situ hybridization studies, embryos were briefly fixed in 4% paraformaldehyde followed by methanol and hydrogen peroxide washes and proteinase-K treatment as described¹. All probes were as described^{1,2}, or derived by PCR and sequenced.

Received 4 May; accepted 13 July 1999.

1. Szeto, D. P. *et al.* Role of the bicoid-related homeodomain factor *Pitx1* in specifying hindlimb morphogenesis and pituitary development. *Genes Dev.* 13, 484-494 (1999).
2. Logan, M. & Tabin, C. J. Role of *Pitx1* upstream of *Tbx4* in specification of hindlimb identity. *Science* 283, 1736-1739 (1999).
3. Lantieri, C., Lamolet, B. & Drouin, J. The bicoid-related homeoprotein *Pitx1* defines the most anterior domain of the embryo and differentiates posterior from anterior lateral mesoderm. *Development* 124, 2807-2817 (1997).
4. Semina, E. V. *et al.* Cloning and characterization of a novel bicoid-related homeobox transcription factor gene, *RIEG*, involved in Rieger syndrome. *Nature Genet.* 14, 392-399 (1996).
5. Gage, P. J. & Camper, S. A. Pituitary homeobox 2, a novel member of the bicoid-related family of homeobox genes, is a potential regulator of anterior structure formation. *Hum. Mol. Genet.* 6, 457-464 (1997).
6. Campione, M. *et al.* The homeobox gene *Pitx2*: mediator of asymmetric left-right signaling in vertebrate heart and gut looping. *Development* 126, 1225-1234 (1999).
7. Piedra, M. E., Icardo, J. M., Albajar, M., Rodriguez-Rey, J. C. & Ros, M. A. *Pitx2* participates in the late phase of the pathway controlling left-right asymmetry. *Cell* 94, 319-324 (1998).
8. Logan, M., Pagan-Westphal, S. M., Smith, D. M., Paganessi, L. & Tabin, C. J. The transcription factor *Pitx2* mediates situs-specific morphogenesis in response to left-right asymmetric signals. *Cell* 94, 307-317 (1998).
9. Yoshioka, H. *et al.* *Pitx2*, a bicoid-type homeobox gene, is involved in a lefty-signaling pathway in determination of left-right asymmetry. *Cell* 94, 299-305 (1998).
10. Mono, C. *et al.* *Lefty-1* is required for left-right determination as a regulator of *Lefty-2* and nodal. *Cell* 94, 287-297 (1998).
11. Ryan, A. K. *et al.* *Pitx2* determines left-right asymmetry of internal organs in vertebrates. *Nature* 394, 545-551 (1998).
12. Mucchielli, M. L. *et al.* Mouse *Orb2/RIEG* expression in the odontogenic epithelium precedes tooth initiation and requires mesenchyme-derived signals for its maintenance. *Dev. Biol.* 189, 275-284 (1997).
13. Semina, E. V., Reiter, R. S. & Murray, J. C. Isolation of a new homeobox gene belonging to the *Pitx/RIEG* family: expression during lens development and mapping to the aphakia region on mouse chromosome 19. *Hum. Mol. Genet.* 6, 2109-2116 (1997).
14. Thomas, T., Yamagishi, H., Overbeck, P. A., Olson, E. N. & Srivastava, D. The bHLH factors, dHAND and eHAND, specify pulmonary and systemic cardiac ventricles independent of left-right sidedness. *Dev. Biol.* 196, 228-236 (1998).
15. Bibben, C. & Harvey, R. P. Homeodomain factor *Nkx2-5* controls left/right asymmetric expression of bHLH gene *eHand* during murine heart development. *Genes Dev.* 11, 1357-1369 (1997).
16. Hogan, B. L. Morphogenesis. *Cell* 96, 225-233 (1999).
17. Oh, S. P. & Li, E. The signaling pathway mediated by the type IIB activin receptor controls axial patterning and lateral asymmetry in the mouse. *Genes Dev.* 11, 1812-1826 (1997).
18. Ericson, J., Nordin, S., Jessell, T. M. & Edlund, T. Integrated FGF and BMP signaling controls the progression of progenitor cell differentiation and the emergence of pattern in the embryonic anterior pituitary. *Development* 125, 1005-1015 (1998).

19. Treier, M. *et al.* Multistep signaling requirements for pituitary organogenesis in vivo. *Genes Dev.* 12, 1691-1704 (1998).
20. Dasen, J. S. *et al.* Reciprocal interactions of *Pit-1* and *GATA-2* mediate signaling gradient-induced determination of pituitary cell types. *Cell* 97, 1-20 (1999).
21. Sheng, H. Z. *et al.* Multistep control of pituitary organogenesis. *Science* 278, 1809-1812 (1997).
22. Peters, H. & Balling, R. Teeth. Where and how to make them. *Trends Genet.* 15, 59-65 (1999).
23. Martinez, S., Crossley, P. H., Cobos, I., Rubenstein, J. L. & Martin, G. R. FGF8 induces formation of an ectopic isthmus organizer and isthmocerebellar development via a repressive effect on *onx2* expression. *Development* 126, 1163-1200 (1999).
24. Boettger, T., Whittier, L. & Kessel, M. FGF8 functions in the specification of the right body side of the chick. *Curr. Biol.* 9, 277-280 (1999).
25. Collignon, J., Varlet, I. & Robertson, E. J. Relationship between asymmetric nodal expression and the direction of embryonic turning. *Nature* 381, 155-158 (1996).
26. Lowe, L. A. *et al.* Conserved left-right asymmetry of nodal expression and alterations in murine sinus inversus. *Nature* 381, 158-161 (1996).

Acknowledgements

We thank E. Olson, B. Hogan, G. Martin, P. Sharp and P. Overbeck for helpful discussions; M. Treier, A. Gleiberman, R. Burgess, A. Ryan and other members of the laboratory for critical advice, data and discussion; E. Olson, B. Hogan, and P. Gruss for critical reagents; M. Ayers for animal handling; P. Myer for her expertise in preparation of illustrations; and M. Fisher for manuscript preparation. P.B. is on leave from the Advanced Biotechnology Center/IST Genoa, Italy, and is supported by the American Italian Cancer Foundation (Bristol-Myers Squibb Foundation). M.G.R. is an Investigator with the Howard Hughes Medical Institute. This work is supported by NIH grants to M.G.R. and J.C.I.B., and the G. Harold and Leila Y. Mathers Charitable Foundation to J.C.I.B.

Correspondence and requests for materials should be addressed to M.G.R. (e-mail: mrosenfeld@ucsd.edu) or J.C.I.B. (e-mail: belmonte@salk.edu).

Human urotensin-II is a potent vasoconstrictor and agonist for the orphan receptor GPR14

Robert S. Ames[†], Henry M. Sarau[†], Johathan K. Chambers[§], Robert N. Willette[‡], Nambi V. Aiyar[‡], Anne M. Romanic[‡], Calvert S. Loudon^{||}, James J. Foley[‡], Charles F. Sauermelch[‡], Robert W. Coatney[§], Zhaohui Ao[‡], Jyoti Disa[‡], Stephen D. Holmes[‡], Jeffrey M. Stadel[‡], John D. Martin[¶], Wu-Schyong Liu[¶], George I. Glover[¶], Shelagh Wilson[¶], Dean E. McNulty[¶], Catherine E. Ellis[¶], Nabil A. Elshourbagy[¶], Usman Shabon[¶], John J. Trill[¶], Douglas W. P. Hay[‡], Eliot H. Ohlstein[‡], Derk J. Bergsma[¶] & Stephen A. Douglas[‡]

Departments of [†] Molecular Biology, [‡] Pulmonary and Cardiovascular Pharmacology, [§] Functional Gene Analysis, ^{||} Pathology, [¶] Laboratory Animal Sciences, [¶] Immunology, [¶] Protein Biochemistry and [¶] Gene Expression Sciences, Smith Kline Beecham Pharmaceuticals, 709 Swedeland Road, King of Prussia, Pennsylvania 19406-0939, USA and Southern Way, Harlow, Essex CM19 5AW, UK

[†] These authors contributed equally to this work

Urotensin-II (U-II) is a vasoactive 'somatostatin-like' cyclic peptide which was originally isolated from fish spinal cords^{1,2}, and which has recently been cloned from man³. Here we describe the identification of an orphan human G-protein-coupled receptor homologous to rat GPR14 (refs 4, 5) and expressed predominantly in cardiovascular tissue, which functions as a U-II receptor. Goby and human U-II bind to recombinant human GPR14 with high affinity, and the binding is functionally coupled to calcium mobilization. Human U-II is found within both vascular and cardiac tissue (including coronary atheroma) and effectively constricts isolated arteries from non-human primates. The potency of vasoconstriction of U-II is an order of magnitude greater than that of endothelin-1, making human U-II the most potent mammalian vasoconstrictor

identified so far. *In vivo*, human U-II markedly increases total peripheral resistance in anaesthetized non-human primates, a response associated with profound cardiac contractile dysfunction. Furthermore, as U-II immunoreactivity is also found within central nervous system and endocrine tissues, it may have additional activities.

In an effort to identify novel G-protein-coupled receptors (GPCRs), we probed a human genomic library with rat GPR14 (SENRA)^{4,5}, an orphan GPCR similar to somatostatin receptors. We isolated a 9-kilobase (kb) genomic clone which encoded a 389-residue human GPCR (75% identity to rat GPR14; Fig. 1). GPR14 messenger RNA was most abundant in the heart and pancreas (no expression was detected in 15 discrete brain regions; see Supplementary Information); however, using quantitative polymerase chain reaction with reverse transcription (RT-PCR), low levels of transcript were detectable in thalamus, superior occipital gyrus and substantia nigra. Additional RT-PCR revealed expression in human cardiac (atria and ventricle) and arterial (aorta) tissue, endothelial (coronary artery and umbilical vein) cells and smooth muscle (coronary artery and aortic) cell lines, but not in vena cava nor in a venous (renal vein) smooth muscle cell line.

Human GPR14 was subcloned into a mammalian expression vector and transfected into HEK-293 cells. In a 'reverse pharmacological approach'^{6,7}, the cells were used to search for a ligand activating GPR14 using a calcium-mobilization assay. Using a fluorescent imaging plate reader (FLIPR), transiently transfected cells were exposed to over 700 known and putative GPCR agonists. We detected a robust calcium-mobilization response in cells transfected with either rat or human GPR14 only upon challenge with goby U-II (effector concentration for half maximum response

(EC₅₀) of 0.78 ± 0.18 and 0.47 ± 0.14 nM, respectively; Fig. 2a). This response was highly selective for goby U-II and was not induced by any of the other ligands we tested. Cells transfected with expression vector alone, or vectors encoding other orphan GPCRs such as GPR7 or GPR8, which are also homologous to the somatostatin receptors⁸, did not respond to goby U-II.

A human GPCR that selectively responded to a non-mammalian neuropeptide indicated the possible existence of a human orthologue. A search of GenBank using the carp U-II sequence⁹ yielded a match to a human expressed sequence tag (EST) with 25% identity to the fish sequence. Using this EST, we isolated a 688-base pair (bp) complementary DNA encoding human U-II (Fig. 3). The deduced propeptide sequence contained an amino-terminal signal sequence (cleaved at residue 17) and three putative polybasic proteolytic cleavage sites (Fig. 3), but varied at the amino terminus from the human U-II propeptide described subsequently in ref. 3, probably as a result of alternative splicing. The mature sequence (ETPDICFW-KYCV) was identical to human U-II (ref. 3), and it retained the cyclic hexapeptide sequence (CFWKYC) that is absolutely conserved across species¹². Expression of the U-II transcript was restricted to the spinal cord and medulla oblongata (see Supplementary Information), consistent with previous reports in fish, frogs and humans¹⁻³.

Human U-II induced concentration-dependent increases in intracellular calcium in a HEK-293 cell line expressing human GPR14 (EC₅₀ = 0.62 ± 0.17 nM, $n = 6$; Fig. 2b). ¹²⁵I-labelled goby U-II bound saturably and with high affinity to membranes prepared from these cells (Fig. 2c; $K_d = 0.43 \pm 0.01$ nM; $B_{max} = 447 \pm 58$ fmol mg⁻¹ protein; $n = 3$). Goby and human U-II displaced the radioligand with comparable affinities

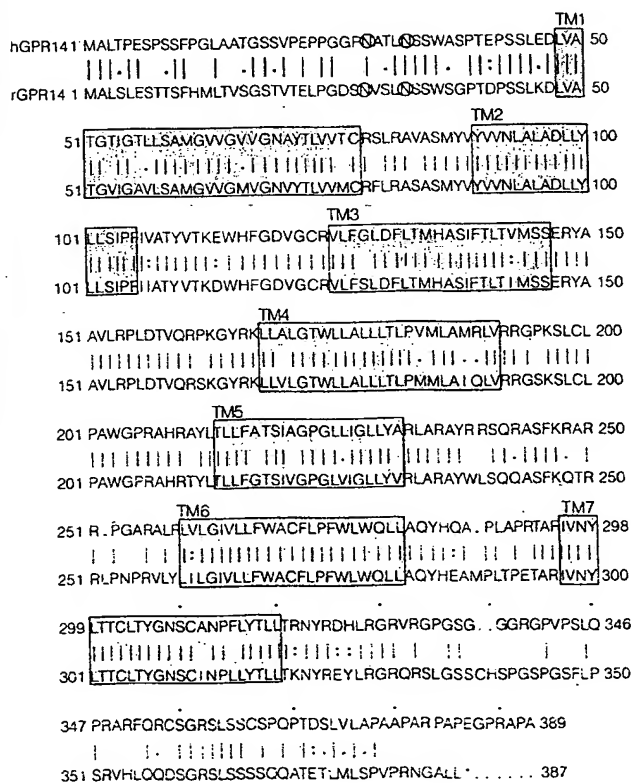


Figure 1 Alignment of rat (r) and human (h) GPR14 polypeptide sequences. The predicted seven transmembrane (TM) spanning regions are shaded and potential N-linked glycosylation sites are circles. GenBank accession number of human GPR14 is AF140631.

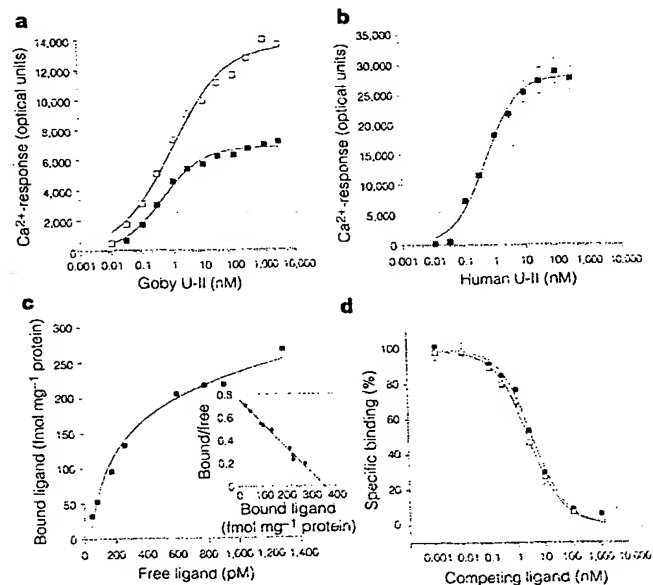


Figure 2 GPR14 is a U-II receptor. **a**, Goby U-II-induced Ca²⁺-mobilization (FLIPR) in HEK-293 cells transiently transfected with rat (filled squares) or human GPR14 (open squares). **b**, Ca²⁺-mobilization response to human U-II in clonal HEK-293 cell lines stably transfected with human GPR14. **c**, Saturation binding isotherm for ¹²⁵I-labelled goby U-II in cell membranes from HEK-293 cells stably transfected with human GPR14 (inset, Scatchard analysis). **d**, Competition binding curves for human (filled squares) and goby U-II (open squares) with human GPR14.

letters to nature

[illegible]

Figure 3 Nucleotide and deduced peptide sequence of human U-II propeptide cDNA. Putative polybasic cleavage sites are shown in bold and underlined. The putative mature human U-II is shown in italics. GenBank accession number is AF140630.

Table 1 Relative contractile potency of human U-II in non-human primates

Vessel	Human urotensin-II -log[EC ₅₀]	Endothelin-1 -log[EC ₅₀]	Relative potency
Arterial tissue			
Left anterior descending coronary	9.39 ± 0.40	8.20 ± 0.32*	15
Left circumflex coronary	9.56 ± 0.05	n.d.	
Mesenteric	9.35 ± 0.26	8.24 ± 0.28*	13
Pulmonary	9.29 ± 0.16	7.84 ± 0.06***	28
Renal	9.59 ± 0.36	8.83 ± 0.24	6
Proximal descending thoracic aorta	8.86 ± 0.24	n.d.	
Distal descending thoracic aorta	9.06 ± 0.22	n.d.	
Distal abdominal aorta	9.37 ± 0.13	n.d.	
Basilar	10.00 ± 0.16	n.d.	
Common carotid	9.16 ± 0.08	n.d.	
Internal mammary	9.30 ± 0.08	n.d.	
Venous tissue			
Portal vein	<7.00	7.00 ± 0.77	
Jugular vein	<7.00	8.88 ± 0.21	

All values are mean \pm s.e.m. ($n = 3-4$). Statistical comparisons made by analysis of variance (post-hoc Fisher's least-squares difference): * $P < 0.05$ and *** $P < 0.001$. n.d., not determined.

($K_i = 2.06 \pm 0.29$ and 1.99 ± 0.23 nM, respectively; Fig. 2d). Hill coefficients for goby and human U-II approximated to unity ($n_{H_i} = 0.8 \pm 0.1$ and 0.9 ± 0.1 , respectively), indicative of interactions with a single, homogeneous population of binding sites. Binding sites for fish U-II are found in rat arterial membranes, although receptor density is extremely low ($2\text{--}20$ fmol mg^{-1} protein¹⁰). We have made similar observations in rat cardiac membranes ($K_d = 0.35$ nM; $B_{\text{max}} = 3.8$ fmol mg^{-1} protein). Although U-II and somatostatin are structurally similar¹¹, human GPR14 functioned as a U-II-selective receptor: $1 \mu\text{M}$ concentrations of somatostatin_{(1-14)}}, urotensin-I, vasopressin, angiotensin-II, MCH, salmon calcitonin and NPY did not compete for binding; neither did they stimulate calcium mobilization in HEK-293 cells expressing human GPR14.

Immunohistochemical evaluation of monkey and human tissue showed (see Supplementary Information) that the vasculature contained U-II-like immunoreactivity. Diffuse immunostaining was observed in human cardiomyocytes and coronary atherosclerotic plaque, where the staining was intense within the lipid-laden smooth muscle/macrophage-rich regions. We noted additional immunoreactivity within spinal cord ventral horn motor neurons and acinar cells lining the thyroid follicles.

Human and goby U-II induced potent and efficacious contractions in the isolated thoracic aorta of rat ($-\log[EC_{50}] = 9.09 \pm 0.19$, $n = 13$; $-\log[EC_{50}] = 9.22 \pm 0.18$, $n = 15$, respectively; Fig. 4a). Human U-II was significantly more potent ($P < 0.001$) than endothelin-1 (ET-1), noradrenaline and serotonin ($-\log[EC_{50}] = 7.90 \pm 0.11$, 7.58 ± 0.11 and 6.27 ± 0.12 , respectively; $n = 11$, 13 and 4 , respectively; Fig. 4a). Thus, U-II is the most potent human vasoconstrictor peptide identified so far (16-fold

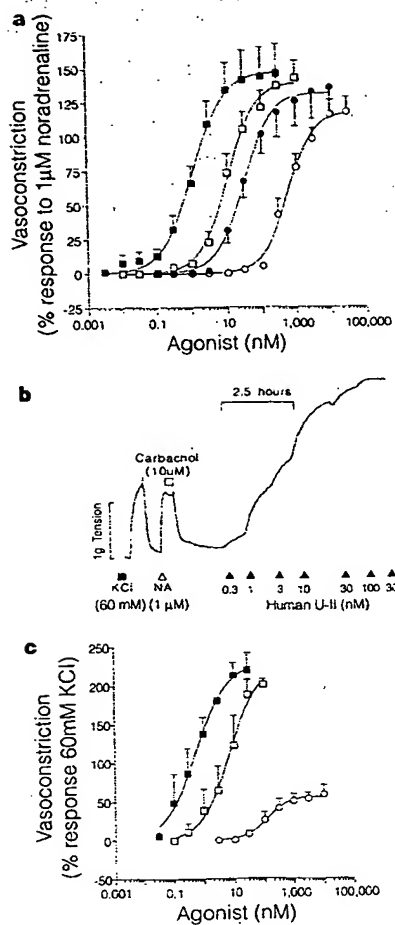


Figure 4 Human U-II is a potent vasoconstrictor. **a**, Concentration-dependent contraction of rat isolated aorta by human U-II (filled squares; $n = 13$), ET-1 (open squares; $n = 11$), noradrenaline (filled circles; $n = 13$) and serotonin (open circles; $n = 4$). **b**, Trace showing concentration-dependent contraction of the primate isolated aorta by human U-II (filled triangles). Responses to standard concentrations of KCl (filled square) and noradrenaline (open triangle) are shown (successful endothelial denudation is shown by the lack of carbachol-induced vasodilation; open square). **c**, Concentration-dependent contraction of the cynomolgus monkey isolated coronary artery ($n = 4$) in response to human U-II (filled squares), ET-1 (open squares) and serotonin (open circles).

more potent than ET-1 in rat).

The vasoconstrictor activity of human U-II was limited to the thoracic aorta in rat: abdominal aorta or femoral and renal arteries did not contract (radioligand binding sites were undetectable in vessels distal to the aortic arch)¹⁰. Consequently, U-II lacks systemic pressor activity in anaesthetized rats upon intravenous (i.v.) administration^{12,13}. In contrast, however, human U-II caused contraction in all non-human primate arterial vessels studied, including both elastic and muscular arteries (Fig. 4b, c). EC₅₀ values were subnanomolar, making human U-II 6–28-fold more potent than ET-1 (Table 1). Unlike ET-1, however, the contractile actions were restricted to the arterial side of the vasculature, consistent with the differential expression of human GPR14 determined by PCR. Thus, the contractile profile of U-II is species-dependent and U-II exhibits an 'anatomically diverse' contractile profile in the arterial vasculature of the primate.

Following this striking *in vitro* profile, we carried out haemodynamic evaluation in anaesthetized monkeys. Systemic administra-

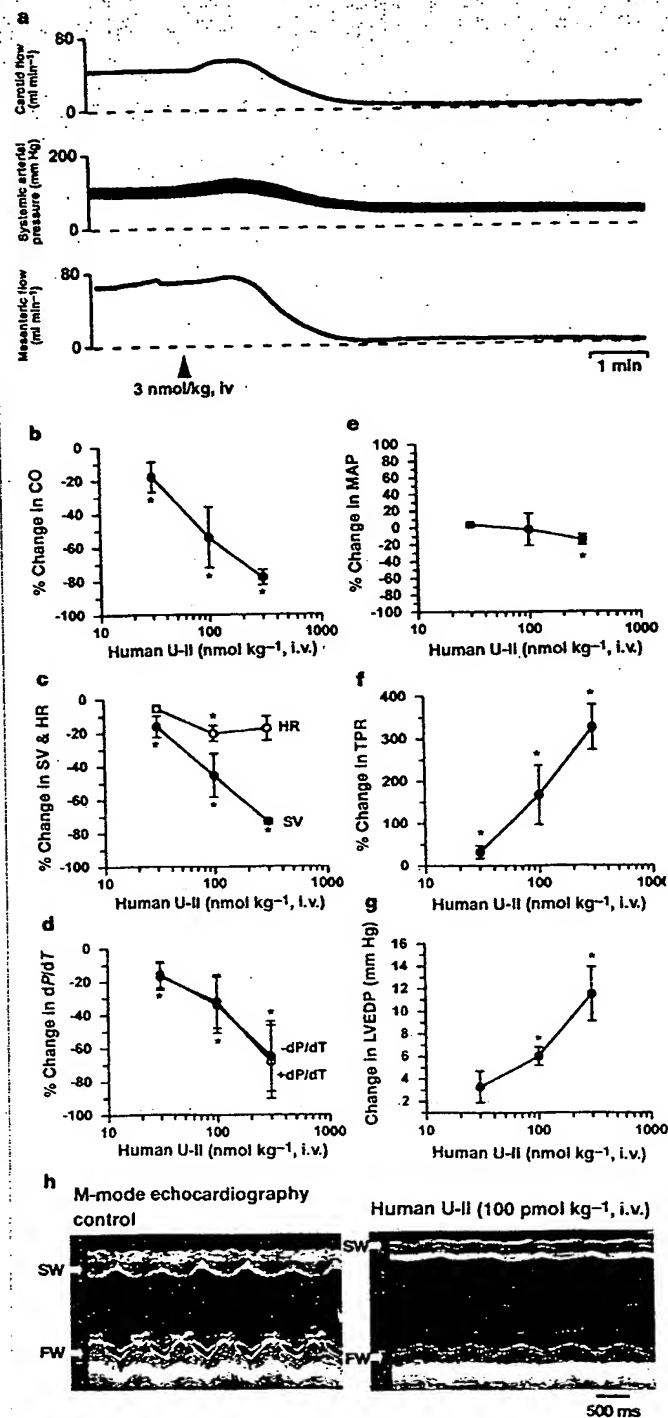


Figure 5 Human U-II produces cardiovascular dysfunction in the anaesthetized monkey. **a**, Fatal circulatory collapse (precipitous falls in systemic pressure and regional flows) induced by bolus i.v. human U-II. Alterations in cardiac output (CO) (**b**), heart rate (HR, open circles) and stroke volume (SV, filled circles) (**c**), myocardial contractility (dP/dt) (**d**), mean arterial pressure (MAP) (**e**), total peripheral resistance (TPR) (**f**) and left ventricular end diastolic pressure (LVEDP) (**g**). *, $P < 0.05$ relative to vehicle ($n = 5$). **h**, M-mode echocardiographic images of the left ventricle before and 7 min after 100 pmol/kg i.v. human U-II show severe attenuation of septal (SW) and free wall (FW) motion.

tion of human U-II elicited a complex dose-dependent haemodynamic response that culminated in severe myocardial depression and fatal circulatory collapse (Fig. 5a). Unusually, a 300 pmol/kg⁻¹ dose of U-II, which induces a 300% increase in total peripheral resistance (indicative of systemic vasoconstriction), did not cause concomitant systemic hypertension. The ability of U-II to induce marked systemic vasoconstriction while also causing catastrophic myocardial contractile dysfunction (for example, 80% decrease in dP/dt and stroke volume) differentiates it from other peptides such as ET-1 and angiotensin-II. For example, 1 nmol/kg⁻¹ ET-1 i.v. (sufficient to elevate total peripheral resistance) is accompanied, not by cardiovascular collapse and systemic hypotension, but rather by a sustained (≤ 1 h) 60 mm Hg increase in arterial pressure¹⁴.

The primate responses were clearly different from those reported in rats^{12,13}. At doses < 30 pmol/kg⁻¹ i.v., human U-II slightly increased cardiac output and reduced regional vascular resistance, with little or no change in arterial blood pressure. In contrast, at doses ≥ 30 pmol/kg⁻¹, human U-II decreased myocardial function and increased vascular resistance. Haemodynamic and echocardiographic analysis demonstrated a dose-dependent reduction in cardiac output (Fig. 5b), the result of mild bradycardia and severely attenuated stroke volume (Fig. 5c). Myocardial contractility was severely depressed, as seen by reductions in dP/dt (Fig. 5d). Despite a marked decrease in cardiac output, sub-lethal doses reduced mean arterial pressure only moderately (Fig. 5e) because of a threefold increase in total peripheral resistance (Fig. 5f). Decreases in regional blood flows and a dose-dependent increase in left ventricular end diastolic pressure (Fig. 5g) indicated systemic vasoconstriction. The severe loss of myocardial contractility was shown by M-mode echocardiography (Fig. 5h) in which grossly attenuated septal and free-wall motion was evident (ultimately, this effect was terminal at doses ranging from 100–3,000 pmol/kg⁻¹). Systemic human U-II administration produced ST segment changes in the electrocardiogram typical of those seen during myocardial ischaemia.

In summary, we have isolated a human GPCR that exhibits the pharmacological characteristics of a U-II receptor. Cells expressing this receptor exhibit high-affinity binding sites for, and respond to, both goby and human U-II. Furthermore, we have demonstrated that U-II is the most potent vasoconstrictor identified so far. Systemic administration is associated with profound cardiovascular collapse. As human U-II-like immunoreactivity is found within cardiac and vascular tissue (including coronary atheroma), this peptide may influence cardiovascular homeostasis and pathology (for example, in ischaemic heart disease and congestive heart failure). Finally, the detection of immunoreactivity within spinal cord and thyroid tissue raises the possibility that U-II may also influence central nervous system and endocrine function in man.

Methods

Cloning

A human genomic placental library (Stratagene) was screened with a ³²P-labelled 1.2-kb PCR-derived clone encoding rat GPR14 (ref. 4), and we identified a positive phage plaque. Two kilobases of insert was sequenced and determined to be homologous to rat GPR14. Human GPR14 was isolated by PCR and subcloned into pCDN (ref. 15). HEK-293 cells were transiently or stably transfected using Lipofectamine Plus (Life Technologies). Using the published fish cDNA sequence⁴, a search of the GenEMBL EST database identified a human cDNA (AA535545) encoding a putative U-II orthologue. After 5'-rapid amplification of cDNA ends (RACE) (placenta and Raji Marathon Ready cDNAs; Clontech), we sequenced and subcloned the resultant products into pCR2.1 (Invitrogen).

Peptide synthesis

Human U-II peptide resin was synthesized (Millipore/Bioscience 9600 synthesizer), cleaved and de-protected before purification by reverse-phase HPLC¹⁸. All other peptides were from Bachem.

Calcium mobilization

We used a microtitre-plate-based calcium-mobilization FLIPR assay, as described previously²², for the functional identification of ligands that activate HEK-293 cells expressing recombinant GPR14. Ligands we tested included micromolar concentrations of all known mammalian neuropeptides and $\geq 10 \mu\text{M}$ concentrations of all known steroid, lipid and amine transmitters.

Radioligand binding

Membranes from HEK-293 cells stably transfected with human GPR14 were pre-coupled to wheatgerm-agglutinin-coated SPA beads (Amersham). Using mono-iodinated goby U-II (¹²⁵I-labelled Tyr¹⁶, chloramine T, 2000 Ci mmol⁻¹; 5 mM MgCl₂, 0.1% BSA, 20 mM Tris-HCl pH 7.4, 25 μg protein; 25 °C), equilibrium binding was measured in 96-well plates (Wallac) after 45 min²⁴. Non-specific binding, determined using 1 μM unlabelled U-II, was ~10% of total binding. There was no specific binding to mock-transfected HEK-293 membranes. We determined protein using biochonic acid (Pierce). Kinetic analysis was by nonlinear least square fitting (GraphPad).

Isolated blood vessel studies

Isolated arterial rings from male Sprague-Dawley rats (400 g) and cynomolgus monkeys (*Macaca fascicularis*) (5 kg) were suspended in organ baths containing Krebs (37 °C; 95% O₂; 5% CO₂)¹⁹. Changes in isometric force were recorded under optimal resting tension. Cumulative agonist concentration-response curves were normalized to 60 mM KCl or 1 μM noradrenaline and fitted to a logistic equation²⁰. Unless stated otherwise, responses were measured in the presence of 10 μM indomethacin using vessels denuded by rubbing (confirmed as a loss of dilator response to 10 μM carbachol).

Haemodynamics and echocardiography

All procedures were performed in accordance with the Guide for the Care and Use of Laboratory Animals (DHSS publication NIH 85-23). Adult male cynomolgus monkeys (5–7 kg) were treated with atropine sulphate (25 μg kg⁻¹ subcutaneous) and anaesthetized with ketamine (10 mg kg⁻¹ intramuscular). After endotracheal intubation, anaesthesia was maintained with 1–3% isoflurane. We prepared the animals for monitoring of systemic haemodynamics. Echocardiography (Doppler, M-mode and 2-D, ATL5000) was carried out at 2–3 min intervals. Vehicle administration (0.9% NaCl) was followed by the cumulative administration of human U-II.

Statistics

Values are expressed as mean \pm s.e.m. n is the number of individual observations made in a particular group. Statistical comparisons were made by one-way analysis of variance (Fisher's protected least-squares difference) and differences considered significant where $P < 0.05$.

Received 8 July; accepted 13 August 1999.

- Bern, H. A., Pearson, D., Larson, B. A. & Nishioka, R. S. Neurohormones from fish tails: the caudal neurosecretory system. I. "Urophysiology" and the caudal neurosecretory system of fishes. *Recent Prog. Horm. Res.* 41, 533–552 (1985).
- Conlon, J. M., Yano, K., Waugh, D. & Hazen, N. Distribution and molecular forms of urotensin II and its role in cardiovascular regulation in vertebrates. *J. Exp. Zool.* 275, 226–238 (1996).
- Coulouarn, Y. et al. Cloning of the cDNA encoding the urotensin II precursor in frog and human reveals intense expression of the urotensin II gene in motoneurons of the spinal cord. *Proc. Natl Acad. Sci. USA* 95, 15863–15868 (1998).
- Marchese, A. et al. Cloning and chromosomal mapping of three novel genes, GPR9, GPR10, and GPR14, encoding receptors related to interleukin 8, neuropeptide Y, and somatostatin receptors. *Genomics* 29, 335–344 (1995).
- Tal, M. et al. A novel putative neuropeptide receptor expressed in neural tissue, including sensory epithelia. *Biochem. Biophys. Res. Commun.* 209, 752–759 (1995).
- Stadel, J. M., Wilson, S. & Bergsma, D. J. Orphan G-protein-coupled receptors: a neglected opportunity for pioneer drug discovery. *Trends Pharmacol. Sci.* 18, 430–437 (1997).
- Libert, E., Vassart, G. & Parmentier, M. Current developments in G-protein-coupled receptors. *Curr. Opin. Cell Biol.* 3, 218–223 (1991).
- O'Dowd, B. F. et al. The cloning and chromosomal mapping of two novel human opioid-somatostatin-like receptor genes, GPR7 and GPR8, expressed in discrete areas of the brain. *Genomics* 28, 84–91 (1995).
- Onsako, S., Ishida, I., Ichikawa, T. & Deguchi, T. Cloning and sequence analysis of cDNAs encoding precursors of urotensin II- α and - γ . *J. Neurosci.* 6, 2730–2735 (1986).
- Itoh, H., McMaster, D. & Lederis, K. Functional receptors for fish neuropeptide urotensin II in major rat arteries. *Eur. J. Pharmacol.* 149, 61–66 (1988).
- Pearson, D. et al. Urotensin II: a somatostatin-like peptide in the caudal neurosecretory system of fishes. *Proc. Natl Acad. Sci. USA* 77, 5021–5024 (1980).
- Gibson, A., Wallace, P. & Bern, H. A. Cardiovascular effects of urotensin II in anesthetized and pithed rats. *Gen. Comp. Endocrinol.* 64, 435–439 (1986).
- Hasegawa, I., Kobayashi, Y. & Kobayashi, H. Vasodepressor effects of urotensin II in rats. *Neuroendocrinol. Lett.* 14, 357–363 (1992).
- Yanagisawa, M. et al. A novel potent vasoconstrictor peptide produced by vascular endothelial cells. *Nature* 332, 411–415 (1988).
- Aiyar, N. et al. Human AT₁ receptor is a single copy gene: characterization in a stable cell line. *Mol. Cell Biochem.* 131, 75–86 (1994).
- King, D. S., Fields, C. G. & Fields, G. B. A cleavage method which minimizes side reactions following

- Fmoc solid phase peptide synthesis. *Int. J. Pept. Protein Res.* 36, 255–266 (1990).
- Chambers, J. et al. Melanin-concentrating hormone is the cognate ligand for the orphan G-protein-coupled receptor SLC-1. *Nature* 400, 261–265 (1999).
- Elshourbagy, N. A. et al. Molecular cloning and characterization of the porcine calcitonin gene-related peptide receptor. *Endocrinology* 139, 1678–1683 (1998).
- Douglas, S. A. & Hiley, C. R. Endothelium-dependent mesenteric vasorelaxant effects and systemic actions of endothelin (16–21) and other endothelin-related peptides in the rat. *Br. J. Pharmacol.* 104, 311–320 (1991).

Supplementary Information is available on Nature's World-Wide Web site (<http://www.nature.com>) or as paper copy from the London editorial office of Nature.

Acknowledgements

We dedicate this Letter to the memory of our friend and colleague, the late J. M. Stadel. We thank D. Ashton, P. Buckley, T. Covatta, J. Culp, G. Dyrko, L. Floyd, P. Hieble, M. Luttmann, G. McCafferty, D. Naselsky, P. Nuthulaganti, P. Ryan and A. Sulpizio for their assistance and comments during the preparation of this manuscript. We thank B. O'Dowd, University of Toronto for the rat GPR14 cDNA clone.

Correspondence and requests for materials should be addressed to R.S.A. (e-mail: bob_ames-1@sbphrd.com). The GenBank accession numbers for human GPR14 and U-II are AF140631 and AF140630, respectively.

A kinase-regulated PDZ-domain interaction controls endocytic sorting of the β 2-adrenergic receptor

Tracy T. Cao*, Heather W. Deacon*, David Reczek†, Anthony Bretscher† & Mark von Zastrow‡

* Department of Biochemistry and Biophysics, University of California, San Francisco, San Francisco, California 94143 USA

† Section of Biochemistry, Molecular and Cell Biology, Cornell University, Ithaca, New York 14853, USA

‡ Program in Cell Biology, Cellular and Molecular Pharmacology and Psychiatry, University of California, San Francisco, San Francisco, California 94143, USA

A fundamental question in cell biology is how membrane proteins are sorted in the endocytic pathway. The sorting of internalized β 2-adrenergic receptors between recycling endosomes and lysosomes is responsible for opposite effects on signal transduction and is regulated by physiological stimuli^{1,2}. Here we describe a mechanism that controls this sorting operation, which is mediated by a family of conserved protein-interaction modules called PDZ domains³. The phosphoprotein EBP50 (for ezrin-radixin-moesin (ERM)-binding phosphoprotein-50)⁴ binds to the cytoplasmic tail of the β 2-adrenergic receptor through a PDZ domain and to the cortical actin cytoskeleton through an ERM-binding domain. Disrupting the interaction of EBP50 with either domain or depolymerization of the actin cytoskeleton itself causes misrouting of endocytosed β 2-adrenergic receptors but does not affect the recycling of transferrin receptors. A serine residue at position 411 in the tail of the β 2-adrenergic receptor is a substrate for phosphorylation by GRK-5 (for G-protein-coupled-receptor kinase-5) (ref. 5) and is required for interaction with EBP50 and for proper recycling of the receptor. Our results identify a new role for PDZ-domain-mediated protein interactions and for the actin cytoskeleton in endocytic sorting, and suggest a mechanism by which GRK-mediated phosphorylation could regulate membrane trafficking of G-protein-coupled receptors after endocytosis.